

# Voltage Control of the Spin Dynamics of an Exciton in a Semiconductor Quantum Dot

J. M. Smith,<sup>1</sup> P. A. Dalgarno,<sup>1</sup> R. J. Warburton,<sup>1</sup> A. O. Govorov,<sup>2</sup> K. Karrai,<sup>3</sup> B. D. Gerardot,<sup>1,4</sup> and P. M. Petroff<sup>4</sup>

<sup>1</sup>*School of Engineering and Physical Sciences, Heriot-Watt University, Edinburgh EH14 4AS, United Kingdom*

<sup>2</sup>*Department of Physics and Astronomy, Ohio University, Athens, Ohio, USA*

<sup>3</sup>*Center for NanoScience and Department für Physik, Ludwig-Maximilians-Universität, 80539 München, Germany*

<sup>4</sup>*Materials Department, University of California, Santa Barbara, California 93106, USA*

(Received 23 September 2004; published 19 May 2005)

We report the observation of a spin-flip process in a quantum dot whereby a dark exciton with total angular momentum  $L = 2$  becomes a bright exciton with  $L = 1$ . The spin-flip process is revealed in the decay dynamics following nongeminate excitation. We are able to control the spin-flip rate by more than an order of magnitude simply with a dc voltage. The spin-flip mechanism involves a spin exchange with the Fermi sea in the back contact of our device and corresponds to the high temperature Kondo regime. We use the Anderson Hamiltonian to calculate a spin-flip rate, and we find excellent agreement with the experimental results.

DOI: 10.1103/PhysRevLett.94.197402

PACS numbers: 78.67.Hc, 73.21.La

The spin of an electron or a hole in a semiconductor nanostructure is very important in determining the electronic and optical properties, and its manipulation has great potential in spintronics and quantum information processing. Crucially, the coherence time of an electron spin is much longer than the time required for coherent manipulation [1]. In the case of an electron-hole pair, an exciton, the spin coherence time is much larger than the radiative recombination time at low temperature [2]. An exciton can be controllably created through absorption of a photon [3,4], and its spin information is transferred to the photon polarization on recombination, but the lifetime is clearly limited by the radiative recombination time, typically 1 ns for self-assembled quantum dots.

In addition to the two bright excitons with angular momentum  $L_z = \pm 1$ , there are two dark excitons with  $L_z = \pm 2$  which do not couple to the light field [5]. In a self-assembled quantum dot, the dark excitons lie a few hundred  $\mu\text{eV}$  below the bright excitons [5,6] and are much longer lived than the bright excitons. Such long lifetimes are attractive for applications, but it is a significant challenge to manipulate dark excitons in a controlled way. In the high symmetry system we study here where the admixture of bright and dark excitons is negligible, the dark excitons are expected to have long spin coherence times. Evidence supporting these assertions is presently very limited, relying on an extrapolation of data recorded under a symmetry-breaking in-plane magnetic field [5].

We report here a novel process which offers control over the conversion of dark into bright excitons in a quantum dot. An electron spin is exchanged with a spin in an adjacent Fermi sea by a coherent Kondo-like tunneling interaction. Our results represent the first time that Kondo physics has been applied to the optical properties of a semiconductor nanostructure, a concept considered only theoretically up until now [7–9]. Significantly, by tuning the energy of the exciton level relative to the

Fermi energy with an external bias, we can control the spin-flip rate.

The InGaAs quantum dots are separated from a highly doped  $n$ -type GaAs contact region by 25 nm of undoped GaAs. By adjusting the bias applied between the back contact and a Schottky gate, we control the electron occupation of the dots [10]. There are clear jumps in the photoluminescence (PL) energy as a function of gate voltage, corresponding to changes in the electron population of the dots [10]. This is a Coulomb blockade phenomenon, as illustrated in Fig. 1(b) where we plot the energies of three states each containing a single hole: the hole-only state,  $h$ , the neutral exciton,  $X^0$ , and the charged exciton,  $X^{1-}$ . The calculations assume a constant lever arm of  $\lambda = 7$  and that the Coulomb energies between two electrons, equivalently between an electron and a hole, are perturbations to the single particle energies, both good approximations for these strongly confined quantum dots [10]. Figure 1(b)

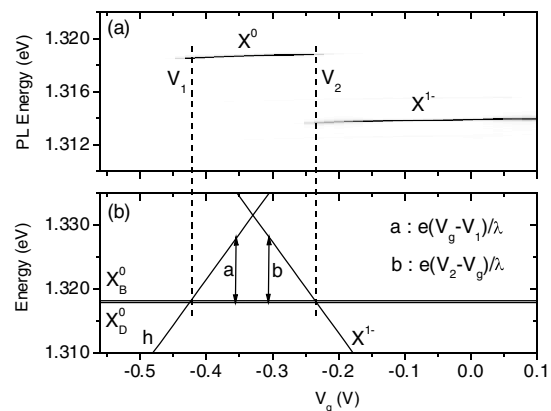


FIG. 1. (a) Gray-scale plot of the PL from a single quantum dot vs gate voltage  $V_g$  at 5 K. White (black) corresponds to 0 (1000) counts. (b) Calculated energy of the initial states vs  $V_g$  with parameters chosen to match (a).

shows how the ground state changes abruptly from  $h$  to  $X^0$  at  $V_g = V_1$  and from  $X^0$  to  $X^{1-}$  at  $V_g = V_2$ , exactly as in the experimental data, Fig. 1(a).

The novel spin-flip process is revealed as a slow component in the decay characteristics of the PL from the  $X^0$  initial state measured on a single quantum dot. Time-resolved photoluminescence (TRPL) is carried out by exciting electron-hole pairs in the wetting layer using a 830 nm, 100 ps pulsed diode laser, and performing time-correlated single photon counting with a silicon avalanche photodiode. The temporal response of the system is 400 ps but by iterative deconvolution we can determine decay times to an accuracy of about 100 ps. The PL is dispersed by a grating spectrometer and detected in a 0.5 meV bandwidth. This is much smaller than the energy shifts on charging but large compared to the small splitting between the two bright states, typically 25  $\mu\text{eV}$  for these quantum dots [4]. The excitation intensity is kept low enough that we observe neither biexciton features in the cw PL nor saturation effects in the TRPL.

Figure 2 shows the PL decay at several bias voltages measured on a single quantum dot. The  $X^{1-}$  decay curves are always single exponentials within the dynamic range of the measurement with a lifetime of typically 0.6 ns. This lifetime corresponds to the radiative lifetime as can be deduced from the known oscillator strength [4]. Hence, the TRPL of  $X^{1-}$  corresponds to a straightforward radiative decay. Conversely, the  $X^0$  decay always shows a second, slower component in addition to the primary component. We can fit the  $X^0$  decay curves extremely well with a biexponential decay. We have verified this striking difference between the  $X^0$  and the  $X^{1-}$  decays on 25 different quantum dots. The crucial spectroscopic difference between  $X^0$  and  $X^{1-}$  is that  $X^0$  has a fine structure but  $X^{1-}$  does not [4]. (For  $X^{1-}$ , the total electron spin is zero such that there is no exchange interaction with the spin- $\frac{3}{2}$  hole.) We therefore associate the two-component  $X^0$  decay with the existence of the dark exciton [11]. In our experiment, fast nongeminate relaxation processes involving the electron reservoir dominate such that we create dark and bright

$X^0$  with equal probability. Direct recombination of the dark exciton can be ruled out as both laser spectroscopy [4] and cw PL [6] on these dots have not revealed any admixture of the dark states with the bright states. Instead, the dark excitons contribute to the signal by undergoing a spin flip, becoming bright and decaying radiatively. Through these arguments, we can be sure that the  $X^0$  TRPL is determined by both radiative decay and exciton spin flip.

The  $X^0$  decay depends strongly on bias, as shown in Figs. 2 and 3. In the center of the  $X^0$  plateau, the primary component has a lifetime of 0.6 ns, exactly the radiative lifetime, and the secondary component has a lifetime of  $\sim 17$  ns and makes a small contribution to the time-integrated signal. Conversely, towards either the low-bias or the high-bias edge of the  $X^0$  plateau, the secondary component has a much smaller and strongly bias-dependent lifetime and makes a significant contribution to the time-integrated signal while the primary lifetime remains at 0.6 ns. In this regime, we associate the secondary lifetime with the exciton spin-flip time.

A comparison of Figs. 3 and 1(b) suggests strongly that the energy separation between the  $X^0$  and the higher lying level, either the hole-only state or the  $X^{1-}$  state depending on bias, determines the dark to bright spin-flip time. We propose that the interaction arises through an electron spin flip involving the Fermi sea, as shown in Fig. 4, with the hole spin remaining unchanged. In terms of an interaction via virtual states, there are two possibilities. In the first case, the electron in the dark exciton tunnels to an empty state close to the Fermi energy in the back contact, leaving the dot in the hole-only state. An electron with opposite spin tunnels into the dot from a filled state creating a bright exciton. This process dominates on the low-bias side of the  $X^0$  plateau. In the second case, which dominates on the

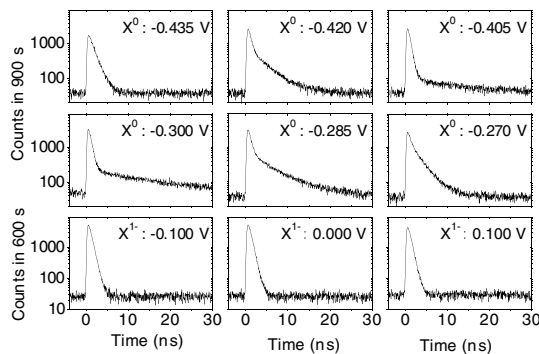


FIG. 2. PL decay curves measured on the quantum dot in Fig. 1(a) for various  $V_g$ . The temperature was 5 K.

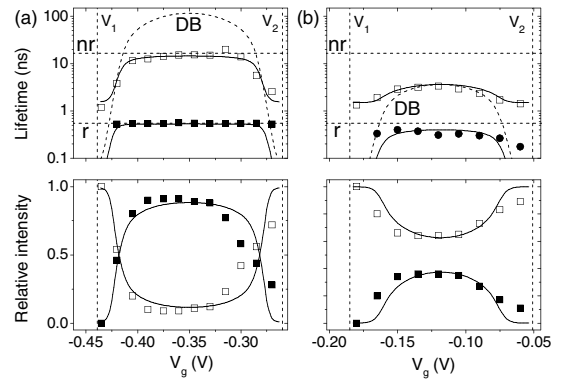


FIG. 3. (a) Lifetimes and relative intensities of the primary (filled symbols) and secondary (open symbols) components of the PL decay vs  $V_g$  for the dot in Figs. 1(a) and 2. (b) As for (a) but for a dot with  $X^0$  emission energy 1.373 eV. The solid lines are the results of the calculations taking  $\gamma_r = 1.8 \text{ ns}^{-1}$ ,  $\gamma_{nr} = 0.06 \text{ ns}^{-1}$ ,  $\delta_{BD} = 0.3 \text{ meV}$ ,  $\Gamma_0 = 50 \mu\text{eV}$  with (a)  $\Delta = 0.07 \text{ meV}$  and (b)  $\Delta = 0.3 \text{ meV}$ . The individual components  $\gamma_r^{-1}$ ,  $\gamma_{nr}^{-1}$ , and  $\gamma_{DB}^{-1}$  are shown by the dashed lines.

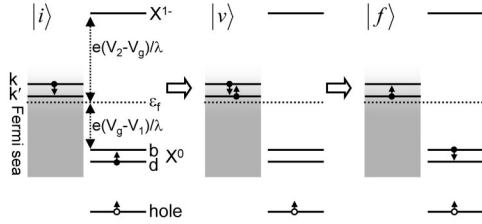


FIG. 4. Schematic representation of the transition of a dark exciton  $d$ , state  $|i\rangle$ , to a bright exciton  $b$ , state  $|f\rangle$ . The splitting between  $b$  and  $d$  is  $\delta_{BD}$ . Two continuum states are considered,  $k$  and  $k'$ , split by  $\delta_{BD}$ . Electrons are labeled with  $\bullet$  with arrows  $\uparrow, \downarrow$  denoting spin. The hole spin is  $+\frac{3}{2}$  and remains the same.

high-bias side of the  $X^0$  plateau, an electron from the Fermi sea tunnels into the dot, converting the dark exciton into  $X^{1-}$ . The electron with opposite spin tunnels into an empty state in the Fermi sea, leaving a bright exciton in the dot. In both cases, energy is conserved by insisting that the energy splitting between the bright and dark excitons is matched by the energy difference between the participating continuum states. We confirm this spin-flip mechanism by demonstrating quantitative agreement with model calculations.

We calculate the dark to bright exciton spin-flip rate  $\gamma_{DB}$  using the Anderson Hamiltonian which describes the interaction of a localized electron with a Fermi sea. Excitation generates predominantly quantum dotlike states provided we are not too close to  $V_g = V_1$  or  $V_2$ . We then treat the tunneling term in the Hamiltonian as a perturbation, calculating the spin-flip rate in the Born approximation. The tunneling term,  $\sum_{k,s} V_k (c_{ks}^\dagger c_s + c_s^\dagger c_{ks})$ , gives a zero result in first order for the spin-flip process. Here,  $V_k$  is the tunneling matrix element,  $c^\dagger$  and  $c$  denote creation and annihilation operators, respectively, and  $s$  is either spin- $\uparrow$  or spin- $\downarrow$ . The Hamiltonian can be transformed by the Schrieffer-Wolf canonical transformation such that all terms to first order in  $V$  disappear. The new Hamiltonian contains several terms to second order in  $V$  but the only significant term for the spin flip is  $\frac{1}{2} \sum_{k,k',s} A V_k V_{k'} c_{k's}^\dagger c_{k-s} c_s^\dagger c_s$  with amplitude,

$$A = \frac{1}{\varepsilon_k - \varepsilon_L} + \frac{1}{\varepsilon_{k'} - \varepsilon_L} + \frac{1}{\varepsilon_L + U - \varepsilon_k} + \frac{1}{\varepsilon_L + U - \varepsilon_{k'}}, \quad (1)$$

where  $\varepsilon_L$  is the energy of the localized state,  $\varepsilon_k$  the energy of the continuum state with wave vector  $k$ , and  $U$  is the on-site Coulomb energy. This term swaps a discrete electron spin with a continuum electron spin and ultimately leads to the Kondo effect. We use this transformed perturbation in first order to calculate  $\gamma_{DB}$ . The calculation involves summing over all possible pairs of continuum states separated by the splitting between the dark and bright states,  $\delta_{BD}$ . The denominators in Eq. (1) result in singularities which we remove by taking into account the dephasing rates of

the initial and final states through an imaginary part to the energies in Eq. (1). Assuming that  $V_k$  is independent of  $k$ ,

$$\gamma_{DB} = \frac{\Delta^2}{h} \int_{\varepsilon} \left| \frac{1}{\varepsilon + e(V_g - V_1)/\lambda + \frac{i}{2}\Gamma} + \frac{1}{e(V_2 - V_g)/\lambda - \varepsilon + \frac{i}{2}\Gamma} \right|^2 \times f(\varepsilon)[1 - f(\varepsilon - \delta_{BD})] d\varepsilon. \quad (2)$$

The Fermi energy  $\varepsilon_f$  is defined to lie at zero energy,  $f(\varepsilon)$  is the Fermi-Dirac function,  $f(\varepsilon) = 1/(e^{\varepsilon/k_B T} + 1)$ , and  $\Delta$  is the tunnel energy given by  $\Delta = 2\pi|V|^2 g(\varepsilon_f)$ ,  $g(\varepsilon)$  being the density of states.  $\Gamma$  is the energy broadening,  $\Gamma = \Gamma_0 + 2\Delta[f[e(V_g - V_1)/\lambda] + f[e(V_2 - V_g)/\lambda]]$ , the first term accounting for dephasing from both electron-hole pair and phonon scattering, the second term accounting for tunneling. Clearly, the product of the Fermi-Dirac functions in Eq. (2) implies that only states within a few  $k_B T$  of  $\varepsilon_f$  contribute to the integral, justifying our assumption that  $V_k$  can be taken as a constant. It now becomes clear that the bright exciton can be converted into a dark exciton by a similar process with the corresponding rate  $\gamma_{BD} = e^{\delta_{BD}/k_B T} \gamma_{DB}$ .

We can estimate  $\Delta$ ,  $\delta_{BD}$ , and  $\Gamma_0$  from the PL spectra. To determine  $\delta_{BD}$ , we measure the PL from more highly charged excitons for which the  $L = 2$  states become bright [6]; we find  $\delta_{BD} = 0.3$  meV for the dots in Fig. 3. For  $V_g$  just larger than  $V_2$ , the electron remaining after recombination tunnels out of the dot such that the spectral linewidth at this voltage is  $2\Delta$ . For the dots in Fig. 3, we find  $\Delta = 0.07$  and  $0.3$  meV. We have confirmed our values for  $\Delta$  through calculations of the tunneling time,  $\tau_t = \Delta/\hbar$ , for quantum dot-continuum tunneling.  $\tau_t$  depends exponentially on the quantum dot ionization energy, estimated to be 95 meV for the dot in Fig. 3(a) from the Coulomb blockade, and on the tunnel barrier thickness, 25 nm.  $\tau_t$  depends relatively weakly on the prefactor to the exponential which contains the vertical confinement, the height and the effective mass which we take to be 220 meV, 3 nm, and  $0.07m_0$ , respectively. This gives  $\tau_t \sim 12$  ps, equivalently  $\Delta = 0.055$  meV, which agrees well with the value from the  $X^{1-}$  PL. Finally, we determine  $\Gamma_0$  to be  $\sim 50$   $\mu$ eV from the  $X^0$  PL linewidth under our experimental conditions. We find that the spin-flip rate depends only weakly on this parameter.

In order to relate the results for the spin-flip processes to the  $X^0$  decay curves we need to model the dynamics of the experiment. We consider three levels: a vacuum state, a dark state with population probability  $n_D$ , and a bright state with population probability  $n_B$ .

$$\begin{aligned} \frac{dn_B}{dt} &= -n_B(\gamma_{BD} + \gamma_{nr} + \gamma_r) + n_D\gamma_{DB}, \\ \frac{dn_D}{dt} &= -n_D(\gamma_{DB} + \gamma_{nr}) + n_B\gamma_{BD}, \end{aligned} \quad (3)$$

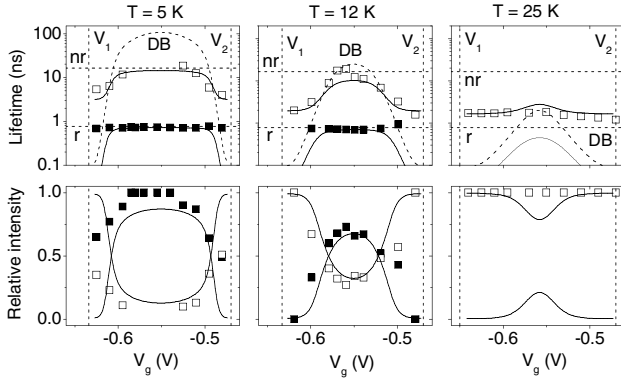


FIG. 5. Primary and secondary decay times and relative intensities for a single quantum dot with  $X^0$  emission energy 1.305 eV (a different dot to Figs. 1–3) for three different temperatures. As in Fig. 3, the solid lines are the fits to the theory taking  $\Delta = 0.08$  meV,  $\gamma_r = 1.3$  ns $^{-1}$ ,  $\gamma_{nr} = 0.06$  ns $^{-1}$ ,  $\delta_{BD} = 0.6$  meV.  $\Gamma_0 = 50, 100$ , and  $120$   $\mu$ eV for 5, 12, and 25 K, respectively. Note that  $V_1$  and  $V_2$  have a small temperature dependence.

where  $\gamma_r$  is the radiative decay rate and  $\gamma_{nr}$  is included to simulate any nonradiative loss. The rate equations yield a biexponential decay, exactly as in the experiment, with rates  $\gamma_{1,2} = P \pm Q$  where  $2P = \gamma_r + 2\gamma_{nr} + \gamma_{DB} + \gamma_{BD}$  and  $2Q = \sqrt{\gamma_r^2 + 2\gamma_r(\gamma_{BD} - \gamma_{DB}) + (\gamma_{DB} + \gamma_{BD})^2}$ . When  $\gamma_r \gg \gamma_{BD}, \gamma_{DB}$ , the two rates are simply  $\gamma_1 \approx \gamma_r + \gamma_{BD} + \gamma_{nr}$  and  $\gamma_2 \approx \gamma_{DB} + \gamma_{nr}$ . In other cases, however, the relationship of the measured rates  $\gamma_{1,2}$  to the radiative, nonradiative, and spin-flip rates is more complicated. Similar results pertain also to the relative time-integrated intensities of the primary and secondary decay components. Given that dark and bright excitons are created equally and that thermalization of the exciton spin takes much longer than a ns [2], we assume equal initial populations of dark and bright excitons.

Figure 3 shows the comparison of the measured lifetimes and relative intensities with the calculations for two dots. In Fig. 3(a), the dot has a relatively low PL energy such that the exciton is strongly confined and the tunnel energy,  $\Delta = 0.07$  meV, is small ( $\tau_t = 9.4$  ps). Conversely, the dot in Fig. 3(b) has a higher PL energy and hence a larger tunnel energy,  $\Delta = 0.3$  meV ( $\tau_t = 2.2$  ps). We adjust only one parameter,  $\gamma_{nr}$ , to fit the data, taking  $\gamma_{nr} = 0.06$  ns $^{-1}$ . Figure 3 demonstrates a remarkable degree of agreement between the theory and the experimental data. For the strongly confined dot, the secondary lifetime depends strongly on the energy separation between the  $X^0$  state and the higher energy state, either the hole-only or  $X^{1-}$ . Near the center of the  $X^0$  plateau, the spin-flip rate is very small, and the nonradiative loss term results in the secondary component showing a maximum lifetime of  $\sim 17$  ns, and a dramatic suppression in intensity relative to the primary component. For the more weakly confined

dot in Fig. 3(b), the spin-flip rate is larger such that the nonradiative loss process is much less important; the secondary lifetime does not saturate and the intensity of the secondary component remains dominant across the  $X^0$  plateau.

Striking confirmation of our interpretation is provided by raising the temperature, as shown in Fig. 5 for a dot with  $\Delta = 0.08$  meV. The main content of Fig. 5 is that we can model the experimental results extremely well simply by changing the temperature in Eq. (2) keeping  $\Delta$  and  $\delta_{BD}$  fixed. Increasing the temperature softens the Fermi-Dirac distribution function and increases the spin-flip rate. At the edges of the  $X^0$  plateau, the spin flip is faster than radiative recombination, the secondary lifetime is independent of bias, and thermal equilibrium is established between the dark and bright states. By 25 K no evidence of a biexponential decay remains.

The origin of the nonradiative loss mechanism is probably related to hole tunneling out of the dots. It varies significantly from dot to dot, with some highly confined dots showing a nonradiative lifetime of at least 50 ns. We have not required a bias-independent spin-flip process to account for any of our results, indicating that the intrinsic spin lifetime of the dark exciton must be more than 50 ns for strongly confined dots.

In conclusion, we report a voltage-dependent spin-flip rate of a quantum dot exciton. The spin-flip rate can be tuned to be larger or smaller than the recombination rate. The mechanism relies on a Kondo-like interaction between a localized electron in the quantum dot and a delocalized electron in the back contact.

This work was funded by EPSRC (UK), Ohio University, and the Volkswagen and Alexander von Humboldt Foundations. J.M.S. was supported by the Scottish Executive and the Royal Society of Edinburgh. We would like to thank Ian Galbraith for helpful discussions.

- 
- [1] M. Kroutvar *et al.*, Nature (London) **432**, 81 (2004).
  - [2] M. Paillard *et al.*, Phys. Rev. Lett. **86**, 1634 (2001).
  - [3] J.R. Guest *et al.*, Phys. Rev. B **65**, 241310 (2002).
  - [4] A. Högele *et al.*, Phys. Rev. Lett. **93**, 217401 (2004).
  - [5] M. Bayer *et al.*, Phys. Rev. Lett. **82**, 1748 (1999).
  - [6] B. Urbaszek *et al.*, Phys. Rev. Lett. **90**, 247403 (2003).
  - [7] A.O. Govorov, K. Karrai, and R.J. Warburton, Phys. Rev. B **67**, 241307 (2003).
  - [8] T.V. Shahbazyan, I.E. Perakis, and M.E. Raikh, Phys. Rev. Lett. **84**, 5896 (2000).
  - [9] K. Kikoin and Y. Avishai, Phys. Rev. B **62**, 4647 (2000).
  - [10] R.J. Warburton *et al.*, Nature (London) **405**, 926 (2000).
  - [11] B. Patton, W. Langbein, and U. Woggon, Phys. Rev. B **68**, 125316 (2003).